HHS Public Access

Author manuscript

Nature. Author manuscript; available in PMC 2014 December 05.

Published in final edited form as:

Nature. 2014 June 5; 510(7503): 152–156. doi:10.1038/nature13279.

Focused Specificity of Intestinal Th17 Cells towards Commensal Bacterial Antigens

Yi Yang[1], **Miriam B. Torchinsky**[1], **Michael Gobert**[1], **Huizhong Xiong**[1], **Mo Xu**[1], **Jonathan L. Linehan**[2], **Francis Alonzo III**[3], **Charles Ng**[1], **Alessandra Chen**[1], **Xiyao Lin**[1], **Andrew Sczesnak**[1], **Jia-Jun Liao**[1], **Victor J. Torres**[3], **Marc K. Jenkins**[2], **Juan J. Lafaille**[1], and **Dan R. Littman**[1,4,*]

[1]The Kimmel Center for Biology and Medicine of the Skirball Institute, New York University School of Medicine, New York, New York, 10016, USA

[2]Department of Microbiology, Center for Immunology, University of Minnesota Medical School, Minneapolis, Minnesota, 55455, USA

[3]Department of Microbiology, New York University School of Medicine, New York, New York, 10016, USA

[4]Howard Hughes Medical Institute, New York University School of Medicine, New York, New York, 10016, USA

Abstract

T-helper-17 (Th17) cells have critical roles in mucosal defense and in autoimmune disease pathogenesis [1-3]. They are most abundant in the small intestine lamina propria (SILP), where their presence requires colonization of mice with microbiota [4-7]. *Segmented Filamentous Bacteria* (*SFB*) are sufficient to induce Th17 cells and to promote Th17-dependent autoimmune disease in animal models [8-14]. However, the specificity of Th17 cells, the mechanism of their induction by distinct bacteria, and the means by which they foster tissue-specific inflammation remain unknown. Here we show that the T cell receptor (TCR) repertoire of intestinal Th17 cells in *SFB*-colonized mice has minimal overlap with that of other intestinal $CD4^+$ T cells and that most Th17 cells, but not other T cells, recognize antigens encoded by *SFB*. T cells with antigen receptors specific for *SFB*-encoded peptides differentiated into RORγt-expressing Th17 cells, even if *SFB*-colonized mice also harbored a strong Th1 cell inducer, *Listeria monocytogenes*, in their intestine. The match of T cell effector function with antigen specificity is thus determined by the type of bacteria that produce the antigen. These findings have significant implications for understanding

*To whom correspondence should be addressed. dan.littman@med.nyu.edu.

Author contributions: Y.Y. and D.R.L. designed the experiments and wrote the manuscript with input from the co-authors. Y.Y., M.B.T., M.X., C.N., A.C., X.L., and J.L. performed most analyses. M.B.T. constructed TCR hybridomas. M.X. developed *SFB*-specific antibodies. M.G., H.X. and J.J.L. did TCR pyrosequencing analysis. J.L.L. and M.K.J. developed tetramers. F.A. and V.J.T. generated transgenic *Listeria*. A.S. performed RNA-seq analysis of *SFB*.

Author information: Reprints and permissions information is available at www.nature.com/reprints. The authors declare no competing financial interests. Readers are welcome to comment on the online version of the paper.

how commensal microbiota contribute to organ-specific autoimmunity and for developing novel mucosal vaccines.

How *SFB* induces Th17 cells and how these cells contribute to self-reactive pathological responses remain key unanswered questions. A recent study, using mice with monoclonal TCRs, suggested that induction of Th17 cells by *SFB* or other microbiota is independent of cognate antigen recognition [15]. To further evaluate mucosal effector T cell induction in a physiological setting, we undertook an examination of the repertoire and specificity of naturally-arising Th17 cells. To facilitate analyzing live Th17 cells, we used *Il-23r*^{GFP} reporter mice [16], as among CD4$^+$ T cells, only this subset expresses IL-23R. We first asked if SILP Th17 cells are in general responsive to gut luminal commensal antigens. GFP$^+$ (Th17) and GFP$^-$ (non-Th17) CD4$^+$ T cells, purified from *Il-23r*$^{GFP/+}$ C57BL/6 (B6) mice that had been colonized with *SFB*, were incubated with splenic antigen-presenting cells (APCs) and autoclaved small intestinal luminal content of mice from the Jackson laboratory (Jax) and Taconic Farms (Tac). We used the measure of forward scatter (FSC) as a surrogate readout for T cell activation. Intriguingly, only Th17 cells mounted a detectable response to Tac antigens (Extended Data Fig. 1a). *SFB* is one of the bacteria unique to Taconic flora [8]. Thus we repeated the assay with fecal material from *SFB*-monoassociated mice (*SFB*-mono antigens) and detected a robust response only among GFP$^+$ cells (Fig. 1a). These cells did not respond to MHCII-deficient APCs loaded with *SFB*-mono antigens, indicating that the activation was dependent on antigen presentation (Extended Data Fig. 1b). *SFB*-mono antigens selectively stimulated total CD4$^+$ T cells from B6 Tac mice, but not those from B6 Jax mice, consistent with *in vivo* priming of *SFB*-specific Th17 cells (Fig. 1b), and any bystander effect in this assay was negligible (Extended Data Fig. 1c). Next, we used an IL-17A ELISPOT assay to quantify the percentage of Th17 cells from *SFB*-colonized mice responding to commensal antigens. GFP$^+$ cells had a relatively weak response towards Jax antigens, but had a robust response towards Tac antigens. Significantly, *SFB* mono-associated mouse fecal antigens stimulated over 60% of the Th17 cells (Fig. 1c). In contrast, there was no response of Th17 cells to fecal material from germ-free mice (data not shown). Thus, the majority of Th17 cells in the SILP of *SFB*-colonized mice react with *SFB*-derived antigens, while a small proportion respond to non-*SFB* antigen, indicating that most Th17 cells are specific for bacteria in the intestinal lumen.

We wished to compare T cell antigen receptor (TCR) repertoires of Th17 cells and those of non-Th17 cells. Using antibodies against a panel of TCR Vβ's, we observed a higher proportion of Vβ14$^+$ T cells in Th17 cells than in non-Th17 cells from the SILP (Extended Data Fig. 2a and 2b). This bias was recapitulated when the CD4$^+$ T cells were stained with antibodies specific for RORγt and IL-17A, two other characteristic markers of Th17 cells (Extended Data Fig. 2c). However, intracellular staining for IFNγ and Foxp3 indicated no Vβ14$^+$ cell bias among Th1 and Treg cells (Extended Data Fig. 2c). To determine if the Vβ14 enrichment of Th17 cells is influenced by microbiota, we compared *SFB*-free B6 Jax mice with *SFB*-colonized B6 Tac mice. The Jax mice had few RORγt$^+$ Th17 cells, and there was no enrichment of Vβ14$^+$ cells among them. In contrast, Jax mice cohoused with Tac mice had increased numbers of lamina propria Th17 cells, which were enriched for Vβ14$^+$

TCRs (Extended Data Fig. 2d), indicating that the Th17 repertoire is shaped by specific microbiota.

We chose to focus on Vβ14$^+$ cells to further elucidate the gut CD4$^+$ T cell repertoire. First, we used pyrosequencing to examine the repertoire of Vβ14$^+$ SILP Th17 and non-Th17 cells from *SFB*-colonized mice. The complementarity determining region 3 (CDR3) of Vβ14 was determined for each cell population from eight *Il-23r*$^{GFP/+}$ mice. Each sample contained a minimum of several hundred unique CDR3 sequences (Extended Data Fig. 3a). Interestingly, the ten most frequently used unique CDR3 sequences accounted for 60% of the Th17 and only 40% of the non-Th17 repertoire (Extended Data Fig. 3b). Furthermore, the dominant CDR3 sequences in individual mice exhibited a clear bias towards either Th17 or non-Th17 cells (Supplementary Table 1). Many of these CDR3 sequences were shared between mice and were enriched either in Th17 or in non-Th17 cells in individual mice (Extended Data Fig. 3c).

The finding that intestinal Th17 cells have a distinct repertoire prompted us to further determine their antigen specificity. Thus, we sorted single T cells from four mice and sequenced their Vβ14 and paired Vα chains (Extended Data Fig. 4a). Notably, each mouse carried some Vβ14 sequences that were present in multiple sorted cells, and these sequences strongly biased towards Th17 or non-Th17 cells (Extended Data Fig. 4b), corroborating our findings from the high-throughput sequencing analysis. To define the antigen specificity of the TCRs from intestinal Th17 and non-Th17 cell clones, we expressed a cohort of nineteen predominant clonotypic TCRs (ten Th17 clones, eight non-Th17 clones, and one neutral clone) in a NFAT-GFP$^+$ hybridoma that can report on TCR signaling [17]. Upon co-culture of the hybridomas with splenic APCs and heat-inactivated mouse intestinal luminal content, several Th17-TCR hybridomas, but not the non-Th17-TCR hybridomas, responded to Tac antigens, but not to Jax antigens (Extended Data Fig. 4c). Furthermore, when *SFB*-mono antigens were used, we detected responses from 7/10 Th17-TCR and the neutral TCR hybridoma, but none of the non-Th17 cell hybridomas (Fig. 2a). These responses were abrogated if the APCs were from MHCII-deficient mice (Extended Data Fig. 4d).

We next sought to identify epitopes recognized by Th17 cell TCRs using a whole- genome shotgun cloning and expression screen, an unbiased approach previously used to identify T cell antigens from other bacteria [18] (Extended Data Fig. 5a). One bacterial clone, designated *3F12-E8*, stimulated 7B8 and four other Th17-TCR hybridomas (Extended Data Fig. 5b, c and d). Based on the recent annotation of the *SFB* genome [19,20], we assigned the 672bp *3F12-E8* insert to an *SFB* gene (*SFBNYU_003340* [19]). We confirmed the specificity by cloning the full-length gene and demonstrating that its product stimulated the aforementioned five TCRs, but not any other TCRs (Fig. 2b, left). We further mapped a minimal epitope that stimulated all five TCRs and a shorter 8 amino acid epitope that stimulated only the 7B8 and 2A6 hybridomas (Extended Data Fig. 5e).

Another expression screen was performed using the 1A7 hybridoma, which along with three other TCRs formed a distinct cluster with an identical Vα and highly similar Vβ14 CDR3 sequences (Extended Data Fig. 6a). A stimulatory clone, designated *2D10-A10* (Extended Data Fig. 6b & c), contained the N-terminal sequence of another *SFB* gene

(*SFBNYU_004990* [19]). We mapped the epitope for the 1A7 hybridoma to 9 amino acids (Extended Data Fig. 6d). Both the full-length gene product and a 9 amino acid peptide stimulated all four TCRs, indicating that these TCRs indeed recognize the same epitope (Fig. 2b, right). However, the single TCR derived from non-Th17 cells (3F4) displayed a much weaker dose-response to peptide antigen than the other TCRs (Extended Data Fig. 6e).

Thus, eight out of eleven Vβ14^{+} Th17-TCR hybridomas recognized two distinct antigens encoded by *SFB* (Fig. 2c). Both proteins are unique to *SFB*, expressed at medium to high level, and predicted to be secreted or at the cell surface (Fig. 2d). Importantly, primary Vβ14^{+} Th17 cells responded to the two immunodominant *SFB* epitopes (Extended Data Fig. 7a). Although Vβ14^{+} cells consistently responded slightly better, Vβ14^{-} Th17 cells were also stimulated by *SFB* (Extended Data Fig. 7b), suggesting that these cells respond to other *SFB* epitopes. An *in silico* search was conducted for potential epitopes within the *SFB* proteome (Extended Data Fig. 7c and 7d), which yielded several more stimulatory peptides (Extended Data Fig. 7e). Among these, peptide N5, also derived from *SFBNYU_003340*, was a strong stimulator of intestinal Th17 cells, activating both Vβ14^{+} cells and Vβ14^{-} cells (Extended Data Fig. 7f). Thus, in the small intestine, *SFB* is the dominant antigen source for polyclonal Th17 cells, but for few, if any, non-Th17 cells.

We then asked what fate is adopted by T cells expressing *SFB*-specific TCRs. We generated 7B8 TCR transgenic mice [21], and transferred naïve T cells from these mice into isotype-marked congenic B6 mice [22]. After one week, we readily detected donor-derived T cells in the SILP of mice that had been exposed to *SFB*, whereas they were completely absent in *SFB*-deficient recipients (Extended Data Fig. 8a). Remarkably, almost all donor-derived cells became positive for RORγt (Fig. 3a). Similar results were obtained upon transfer of T cells from two other TCR (1A2 and 5A11) transgenic strains into *SFB*-colonized recipient mice (Extended Data Fig. 8b). The donor-derived T cells lacked expression of the transcription factors associated with alternative CD4 T cell programs (e.g. Foxp3, GATA3, and T-bet) (Extended Data Fig. 8c).

To visualize endogenous *SFB*-antigen-specific T cells, we produced MHCII-tetramers containing peptide A6 from *SFBNYU_003340* (3340-A6 tetramer) [23]. The I-A^{b}/3340-A6 tetramer specifically stained GFP^{+} SILP CD4^{+} T cells from *SFB*-colonized *IL-23R*$^{GFP/+}$ mice (Extended Data Fig. 8d). Furthermore, a sizable population of I-A^{b}/3340-A6 tetramer-positive cells was present in B6 Tac, but not in B6 Jax mice (Extended Data Fig. 8e), and these cells were uniformly RORγt positive, indicating that they were *SFB*-elicited Th17 cells (Fig. 3b).

We next aimed to determine whether polarization of the antigen-specific Th17 cells in response to *SFB* colonization is dictated by the nature of the antigenic protein or properties of the microbe. *Listeria monocytogenes*, an enteric pathogenic bacterium that also colonizes the small intestine, typically elicits a Th1 response [24]. Mice were orally infected with *L. monocytogenes* expressing *SFBNYU-003340* (*Listeria-3340*) (Extended Data Fig. 8f) or *SFB* before intravenous transfer of *7B8Tg* T cells. *7B8Tg* T cells accumulated in the SILP of both sets of mice, but, importantly, they expressed T-bet rather than RORγt when the hosts were colonized with *Listeria-3340* (Fig. 3c).

To further investigate a relationship between the fate of SILP T helper cells and the bacterial origins of antigens, we transferred *7B8Tg* T cells into mice that were colonized with both *SFB* and *Listeria* and simultaneously tracked $CD4^+$ T cell responses specific for both bacteria in the SILP using the $Ly5.1^+$ congenic marker for *7B8Tg* cells and LLO-tetramers that stain endogenous *Listeria*-specific T cells derived from the host (Extended Data Fig. 9a). In the presence of both Th17- and Th1-inducing bacteria, *7B8Tg* T cells expressed RORγt, but not T-bet, whereas LLO-$tetramer^+$ cells expressed T-bet, but not RORγt (Fig. 4a and Extended Data Fig. 9b and c). This result is in contrast to the Th1 polarization of TCR transgenic T cells specific for the commensal CBir1 flagellin antigen observed upon infection with the protozoan parasite *Toxoplasma gondii* [25], a Th1-inducing intestinal pathogen. This suggests that, unlike CBir1-encoding *Clostridia*, *SFB* is endowed with the ability to direct a dominant signal specialized for induction of Th17 cells.

SFB colonization of the small intestine is potentially beneficial, attenuating pathogenic bacteria-induced colitis [8], but it can also trigger or exacerbate systemic autoimmune disease [10,11], raising the question as to whether *SFB*-specific Th17 cells can circulate beyond the small intestine. We examined the colons and spleens of *SFB*-positive recipients of *7B8Tg* naïve T cells, and found these cells in both organs. Importantly, more than 80% of these *SFB*-specific T cells in colon and 40% in spleen expressed RORγt (Fig. 4b). Consistent with this result, staining of endogenous T cells from Tac mice revealed 3340-A6 tetramer-positive cells in the large intestine and most of these cells expressed RORγt (Extended Data Fig. 10a and b).

Thus, our results indicate that intestinal antigen-specific $CD4^+$ T cells differentiate to become either Th1 or Th17 cells, depending on which luminal bacterium delivers the antigen. We would like to propose a deterministic model for T helper cell differentiation whereby the bacterial context of cognate antigen delivery dictates the fate of the antigen-specific T cells (Fig. 4c). Our work opens the way towards elucidating the mechanisms of Th17 cell induction by microbiota and of how gut-induced Th17 cells can contribute to distal organ-specific autoimmune disease. In addition, it serves as a guide for future studies of human commensal-specific pro-inflammatory T cells that are thought to contribute to autoimmune diseases such as rheumatoid arthritis [26]. Finally, the demonstration of controlled polarized T cell responses towards commensal bacteria offers the potential for novel approaches towards mucosal vaccination.

Methods Summary

Mice

All mice were housed in the animal facility of The Skirball Institute of Biomolecular Medicine at the New York University School of Medicine. Experimental protocols were approved by the Institutional Animal Care and Use Committee. C57BL/6 mice were purchased from Taconic Farm (B6 Tac) or the Jackson Laboratory (B6 Jax). *Il-23r*^{GFP} mice [16], a gift from M. Oukka (Seattle, Children's Hospital), were maintained by breeding with B6 Tac mice. *7B8Tg*, *1A2Tg* and *5A11Tg SFB*-specific TCR transgenic (Tg) mice were generated as previously described [21] and kept with *SFB*-minus flora. For adoptive transfer,

naive Tg T cells ($CD62L^{hi}$ $CD44^{lo}$ $V\beta14^{+}$ $CD4^{+}$ $CD3^{+}$) were sorted from the spleen and were injected intravenously into congenic recipient mice [22].

Generation of TCR hybridomas

Retroviruses carrying an expression cassette encoding TCRα, TCRβ, and CD4 were used to infect the NFAT-GFP $58\alpha^{-}\beta^{-}$ hybridoma cell line [17].

Construction and screen of whole-genome shotgun library of *SFB*

The shotgun library was prepared with a procedure modified from a previous study [18]. The library is estimated to contain 10^4 clones. The expression of exogenous proteins was induced by IPTG for 4 hours. For antigen screening, pools of heat-killed bacteria (~30 clones per pool) were added to a co-culture of APCs and hybridomas.

MHCII tetramer production and staining

MHCII/3340-A6 tetramer was produced as previously described [23]. SILP T cells were incubated at room temperature for 60 min with fluorochrome-labeled tetramer (10 nM) before staining with relevant antibodies at 4°C.

Heterologous expression of *SFBNYU_003340* in *Listeria monocytogenes*

The entire coding region of *SFBNYU_003340*, including its predicted signal sequence, was sub-cloned into the *Listeria* expression vector pIMK2 [27]. The resultant plasmid was transformed into electrocompetent *Listeria monocytogenes* strain *10403S-inlA^{m}* and plated on selective medium containing kanamycin (50 μg/ml) [28].

Methods

Mice

C57BL/6 mice were purchased from Taconic Farm (B6 Tac) or Jackson Laboratory (B6 Jax). *Il-23r^{GFP}* mice [16] were kindly provided by Dr. Mohammed Oukka (Seattle, Children's Hospital) and maintained by breeding with B6 Tac mice. Ly5.1 mice (*B6.SJL-Ptprca Pepcb/BoyJ*) and MHCII-deficient mice (*B6.129S2-H2$^{dlAb1\text{-}Ea}$/J*) were from Jackson Laboratory.

Antibodies and flow cytometry

The following antibodies were from eBiosciences, BD Pharmingen or BioLegend: Vβ2 (B20.6), Vβ3 (KJ25), Vβ4 (KT4), Vβ5 (MR9-4), Vβ6 (RR4-7), Vβ7 (TR310), Vβ8 (F23.1), Vβ8.1/8.2 (MR5-2), Vβ8.3 (8C1), Vβ10 (B21.5), Vβ11 (CTVB11), Vβ12 (MR11-1), Vβ14 (14-2), CD3 (145-2C11), CD4 (RM4-5), CD25 (PC61), Ly5.1 (A20), Ly5.2 (104), MHCII (M5/114), RORγt (AFKJS-9 or B2D), FOXP3 (FJK-16s), T-bet (eBio4B10), GATA3 (TWAJ), IL-17A (eBio17B7) and IFNγ (XM61.2). Flow cytometric analysis was performed on an LSR II (BD Biosciences) or an Aria II (BD Biosciences) and analyzed using FlowJo software (Tree Star). DAPI (Sigma) was used to exclude dead cells.

T cell preparation and staining

Small intestine lamina propria were minced and then incubated for 30 min at 37°C with collagenase D (1mg/ml; Roche), dispase (0.05U/ml; Worthington) and DNase I (100μg/ml; Sigma). Lymphocytes were collected at the interface of a 40%/80% Percoll gradient (GE Healthcare). Cells were stained for surface markers, followed by fixation and permeabilization (eBioscience).

Calculating enrichment scores

An enrichment score for a given Vβ in IL-23R (GFP)$^+$ cells is defined as the equation of (% of Vβ$^+$ cells in the GFP-positive fraction) / (% of Vβ$^+$ cells in the GFP-negative fraction). *e.g.* for Extended Fig. 2b, Vβ14 enrichment was calculated as (7.45/ (7.45+26.2))/ (4.48/ (4.48+61.8)) or 3.3. A score > 1 means a positive enrichment and a score ≈ 1 means no enrichment.

High throughput TCR sequencing

The SILP cells from *Il-23r*$^{GFP/+}$ mice were stained for surface markers and Vβ14$^+$ CD4$^+$ T cells were sorted on the Aria II. For each sample, we collected about 2 × 10^4 cells (2.17±0.43 × 10^4 cells for GFP$^+$ Th17 cells and 2.38±0.54 × 10^4 cells for GFP$^-$ non-Th17 cells). Cells were lysed in Trizol reagent (Invitrogen) and RNA was extracted following the manufacture's instruction. RNA precipitation was aided with GlycoBlue (Invitrogen). cDNAs were prepared with a reverse transcription kit (USB). Vβ14 PCRs were performed using barcoded oligos. PCR products from 16 samples were quantified on Nanodrop. Equal amounts of barcoded PCR product were mixed and sequenced using a 454 GS Junior system (Roche). The raw sequencing data was first aligned using the high-throughput analysis tool provided by IMGT [29]. We obtained 6647±954 reads for Th17 cells and 5573±889 reads for non-Th17 cells. CDR3 usage was further computed with Perl-based scripts developed in-house. The Th17 samples had 340-772 unique Vβ14 CDR3 sequences and the non-Th17 samples had 849-2148 unique Vβ14 CDR3 sequences.

Single cell TCR sequencing

The SILP cells from *Il-23r*$^{GFP/+}$ mice were stained for surface markers. GFP$^+$ and GFP$^-$ Vβ14$^+$ CD4$^+$ T cells were sorted on the BD Aria II and deposited at one cell per well into 96-well PCR plates preloaded with 5μl reverse transcription mix (USB). Immediately after sorting, whole plates were incubated at 50°C for 60 min for cDNA synthesis. Half of the cDNA was used for Vβ14 PCR using forward primer 5′-ACGACCAATTCATCCTAAGCAC -3′ and reverse primer 5′-AAGCACACGAGGGTAGCCT -3′. To retrieve Vα sequences, the other half of cDNA was preamplified for 16 cycles using a mix of twenty-one forward primers [30] (each modified by adding a 5′ extended anchor sequence: TAATACGACTCACTATAGGG) and a reverse primer 5′- CATGTCCAGCACAGTTTTGTCAGT -3′. The primary Vα PCR products were diluted and subjected to a second round PCR using forward primer 5′-TAATACGACTCACTATAGGG -3′ and reverse primer 5′-GTCAAAGTCGGTGAACAGGC -3′. PCRs were performed in a Lightcycler 480 (Roche). PCR products were cleaned up with ExoSap-IT reagent (USB) and Sanger sequencing was

performed by Macrogen. In nearly all cases, for cells with the same Vβ14 sequence, we retrieved a single unique Vα sequence, indicating that these cells were clonotypically identical.

Generation of TCR hybridomas

The NFAT-GFP 58α $^{-}$β^{-} hybridoma cell line [17] was kindly provided by Dr. Kenneth Murphy (Washington University, St. Louis). To reconstitute TCRs, we used a self-cleavage sequence of 2A to link cDNAs of TCRα and TCRβ generated from annealing of overlapping oligos (TCRα-p2A-TCRβ) and shuttled the cassette into a modified MigR1 retrovector in which IRES-GFP was replaced with IRES-mCD4. Then retroviral vectors were transfected into Phoenix E packaging cells using Lipofectamine 2000 (Invitrogen). Hybridoma cells were transduced with viral supernatants in the presence of polybrene (8μg/ml) by spin infection for 90 min at 32°C. Transduction efficiencies were monitored by checking mCD3 surface expression on day 2. We generated nineteen hybridomas for predominant clonotypic TCRs whose Vα and Vβ sequences were retrieved from single-cell TCR sequencing (# of Vβ ≥ 6 for Th17 biased clones, and # of Vβ ≥4 for Non17 biased clones, # of Vα ≥ 3. Note that a single unique Vα was identified for every Vβ). We also generated the OTII hybridoma using TCR sequences kindly provided by Dr. Francis Carbone (chicken ovalbumin antigen-specific, I-A^{b} restricted).

Assay for hybridoma activation

To prepare antigen-presenting cells, splenocytes from B6 mice that were injected i.p. with 8 × 10^{6} FLT3-B16 melanoma cells 10 days before were positively enriched for CD11c^{+} cells using MACS LS columns (Miltenyi). 1 × 10^{4} hybridoma cells were incubated with 2 × 10^{5} APCs and autoclaved antigens from intestinal luminal contents or fecal material for two days. GFP induction in the hybridomas (CD3^{+} fraction) was analyzed by flow cytometry.

Construction and screen of whole-genome shotgun library of *SFB*

The shotgun library was prepared with a procedure modified from a previous study [18]. In brief, genomic DNA was purified from the feces of *SFB*-monoassociated mice by phenol:choloroform extraction. DNA was subjected to whole-genome amplification with the REPLI-g kit (Qiagen) following the manufacturer's instructions. Amplified materials were partially digested with Sau3A (NEB), then ligated with the BamHI-linearized pGEX-4T1 expression vector (GE Healthcare). Ligation products were introduced into competent Stbl3 cells (Invitrogen). To ensure the quality of the library, we sequenced the inserts of randomly picked colonies. All the sequences were mapped to the *SFB* genome. The library is estimated to contain 10^{4} clones. We grew bacteria in 96-well deepwell plates (VWR) with AirPort microporous cover (Qiagen). The expression of exogenous proteins was induced by IPTG for 4 hours. Then bacteria were heat killed by incubating at 70°C for 1 hour, and stored at -20°C until use. For antigen screens, pools of bacterial clones (∼30 clones per pool) were added to a co-culture of APCs and hybridomas. Clones within the positive pools were screened individually against the hybridoma bait. Finally, the inserts of positive clones were subjected to Sanger sequencing. The sequences were blasted against the *SFB* genome and aligned to annotated open reading frames.

Epitope mapping

We expressed overlapping fragments spanning the active ORF using the pGEX-4T1 bacterial expression system, and colonies were used to stimulate the relevant hybridoma. This process was repeated until we identified minimal fragments conferring antigenicity. The mapping was further verified by stimulating hybridomas with synthetic peptides (Genescript).

RNA-seq analysis of the *SFB* transcriptome

Wild-type B6 mice from Jackson Laboratory or Taconic Farm, confirmed for the presence or absence of *SFB* by qPCR [19], were used for microbiome transcriptome analysis. Within five minutes after sacrifice, the terminal ileum of each mouse was resected and luminal contents were squeezed with sterile forceps into a mortar cooled with liquid nitrogen. 1 ml nuclease-free TE was washed through the ileum into the mortar. The total luminal contents and washing were then ground to a fine powder with a pestle cooled with liquid nitrogen and kept on dry ice. The powder was then transferred to 15 mL Trizol (Life Technologies) in a 50 mL falcon tube and vortexed. The manufacturer's protocol was then used to obtain RNA. The resulting RNA was extracted twice with acid phenol-chloroform, precipitated, treated with Ambion Turbo DNA-free, and cleaned-up with an RNeasy column to yield RNA with an undetectable concentration of DNA by Qubit. A portion of this RNA was treated once with Epicentre's Ribo-Zero rRNA removal kit, using equal volumes of specific oligos from the Meta-bacteria and Human/mouse/rat kits. An Illumina RNA-seq library was prepared from these samples using a previously-described strand-specific Nextera protocol. The resulting reads were aligned to the SFBNYU genome with Bowtie [31] and transcript abundance was estimated using Cufflinks [32] with default parameters.

Production of anti-*SFB* antibody and immunostaining

The cDNA fragments corresponding to amino acids 43-359 (3340N) and 734-1060 (3340C) of *SFBNYU_003340* were cloned into the pGEX6p1 expression vector. Recombinant proteins fused to N-terminal GST were expressed in *E.coli* BL21, purified with Glutathione sepharose 4B (GE), and were released with PreScission protease (GE). The flowthrough fractions containing polypeptides without the GST tag were collected as immunogen. Rabbit polyclonal antibodies against both polypeptides were raised by Covance. For immunostaining, bacteria were fixed with 2% paraformaldehyde, followed by washing with 0.5% TritonX-100. Bacteria were incubated sequentially with primary antibody (1:1 mix of the two rabbit-anti-3340 antibodies) and PE-conjugated goat anti-rabbit antibody.

Activation of polyclonal SILP Th17 cells

GFP^+ and GFP^- SILP $CD4^+$ T cells sorted from *Il-23r*$^{GFP/+}$ mice were incubated with 2×10^5 APCs ($CD11c^+$ cells purified from the spleen) and indicated stimuli in complete RPMI medium supplemented with IL-2 (10u/ml) and IL-7 (5ng/ml) for 2∼3 days. Cells were harvested and stained with Vβ-specific antibodies. Forward scatter increment, as readout for cell activation, was analyzed by FACS.

IL-17A ELISPOT assay

IL-17A ELISPOT was performed with a Mouse/Rat IL-17A ELISPOT Ready-SET-Go! kit (eBioscience). Dots were automatically enumerated with ImmunoSpot software (Version 5.0)

MHCII tetramer production and staining

I-A^b/3340-A6 tetramer was produced as previously described [23]. Briefly, QFSGAVPNKTD, an immunodominant epitope from *SFBNYU_0033400*, covalently linked to I-A^b via a flexible linker, was produced in Drosophila S2 cells. Soluble pMHCII monomers were purified, biotinlyated, and tetramerized with PE- or APC- labeled streptavidin. To stain endogenous cells, SILP cells were first resuspended in FACS buffer with FcR block, 2% mouse serum and 2% rat serum. Then tetramer was added (10 nM) and incubated at room temperature for 60 min. Cells were washed and followed by regular staining at 4°C. I-A^b/2W and I-A^b/LLO tetramers were previously described [23, 33].

Generation of *Th17-TCRTg* mice

TCR sequences of 7B8, 1A2 and 5A11 were cloned into the pTα and pTβ vectors kindly provided by Dr. Diane Mathis [21]. TCR transgenic animals were generated by the Rodent Genetic Engineering Core at the New York University School of Medicine. Positive pups were genotyped by PCR and kept on *SFB*-minus flora.

Adoptive transfer

Spleens from *7B8Tg* mice were harvested and disassociated. Red blood cells were lysed using ACK lysis buffer (Lonza). Naive Tg T cells ($CD62L^{hi}$ $CD44^{lo}$ $V\beta14^+$ $CD4^+$ $CD3^+$) were sorted on a BD Aria II. Cells were transferred into congenic Ly5.1 recipient mice by retro-orbital injection. In some experiments, we used Ly5.1/Ly5.2 TCRTg mice as donor and transferred naive Tg T cells to congenic Ly5.2 recipient mice.

Heterologous expression of *SFBNYU_003340* in *Listeria monocytogenes*

To generate strains of *L. monocytogenes* that express the *SFBNYU_003340* antigen, the entire coding region including its predicted signal sequence was PCR-amplified from a plasmid containing the *SFBNYU_003340* gene. The resultant PCR product was digested and sub-cloned into the *Listeria* expression vector pIMK2 (provided by Colin Hill), allowing the gene to be expressed under the synthetic promoter P_{help} (High expression promoter in *L.M.*) [27]. The resultant plasmid designated pIMK2-3340 was transformed into electrocompetent *Listeria monocytogenes* strain *10403S-inlA*^{m} (provided by Nancy E. Freitag) and plated on selective medium containing Kanamycin (50 μg/ml) [28]. pIMK2 is a derivative of the plasmid pPL2 and stably integrates in single copy within the $tRNA^{Arg}$ gene following electroporation [34]. The integrity of the *SFBNYU_003340* gene was validated by PCR and expression confirmed by coomassie staining of *L. monocytogenes* exoproteins.

Oral infection with *SFB* and *L. monocytogenes*

For *SFB* colonization, we dissolved in sterile PBS fresh fecal pellets collected from *Il-23r*$^{GFP/GFP}$ *RAG2*$^{-/-}$ mice that have highly elevated levels of *SFB*, and infected mice by

oral gavage. For *L. monocytogenes* colonization, we grew *Listeria-3340* and *Listeria-empty* in brain heart infusion medium and infected mice orally with 1×10^9 c.f.u.

Bioinformatic analysis

Protein predictions were made by bioinformatic tools, including Psort (Version 3.0) [35] and Cello (Version 2.5) [36] for localization prediction, and IEDB (Immune Epitope Database) for MHCII binding affinity prediction.

Statistical analysis

All analyses were performed using GraphPad Prism (Version 6.0). Differences were considered to be significant at *P* values <0.05.

Extended Data Legends

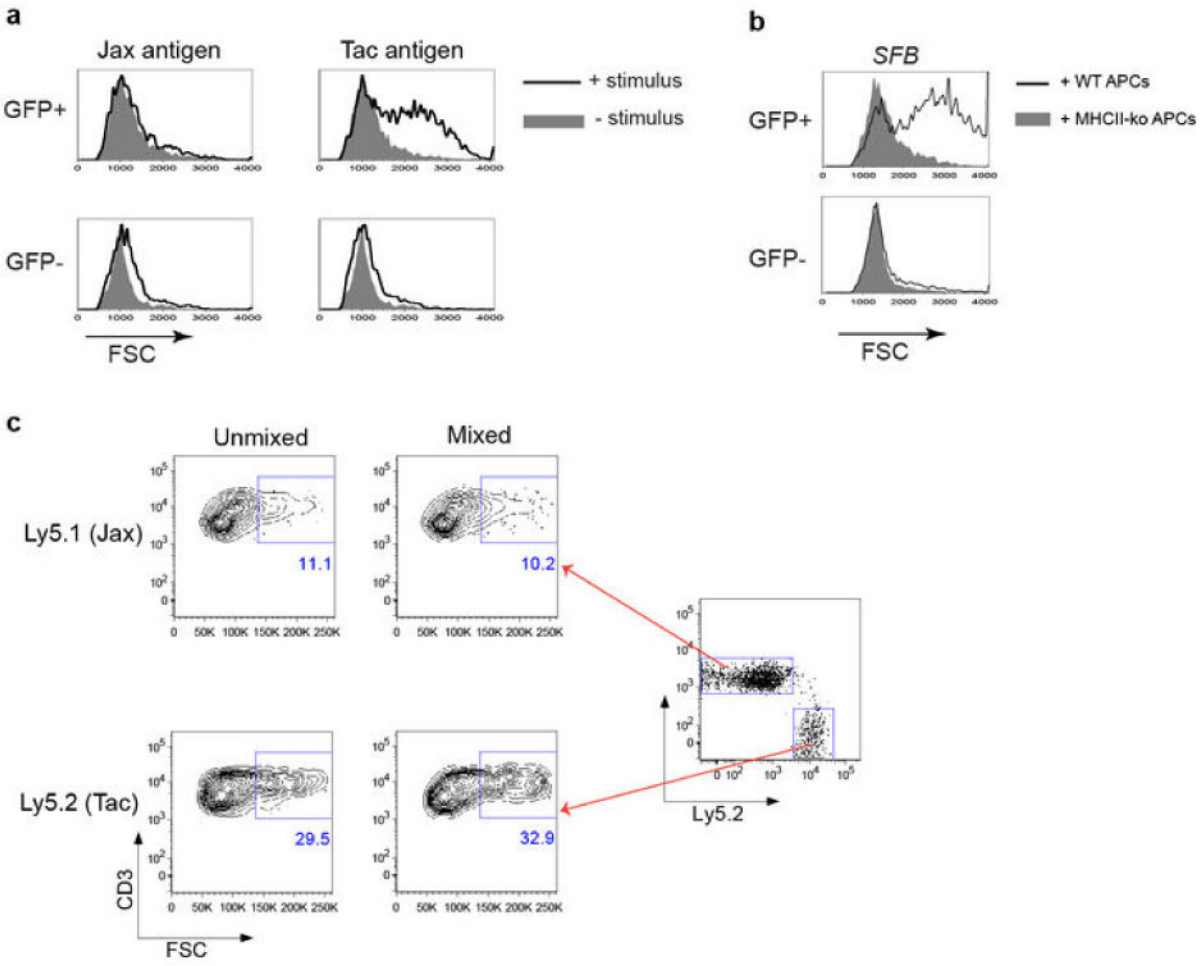

Extended Data Fig. 1. Stimulation of SILP Th17 cells requires intestinal microbiota antigen presentation

(a) Intestinal GFP$^+$ CD4$^+$ T cells from *Il-23r*$^{GFP/+}$ mice stimulated with fecal material from Jax and Tac mice in the presence of syngeneic splenic APCs. Forward scatter was evaluated

after 2 days. **(b)** Th17 cell activation by fecal material from *SFB*-monoassociated mice in the presence of APCs sufficient (WT) or deficient (KO) for MHC class II. **(c)** Evaluation of potential activation of bystander CD4$^+$ T cells upon stimulation with *SFB* antigen. SILP CD4$^+$ T cells from mice with Jax flora (Ly5.1) and Taconic flora (Ly5.2) were co-cultured or stimulated separately with APCs and *SFB*-monoassociated fecal material, and FSC was evaluated.

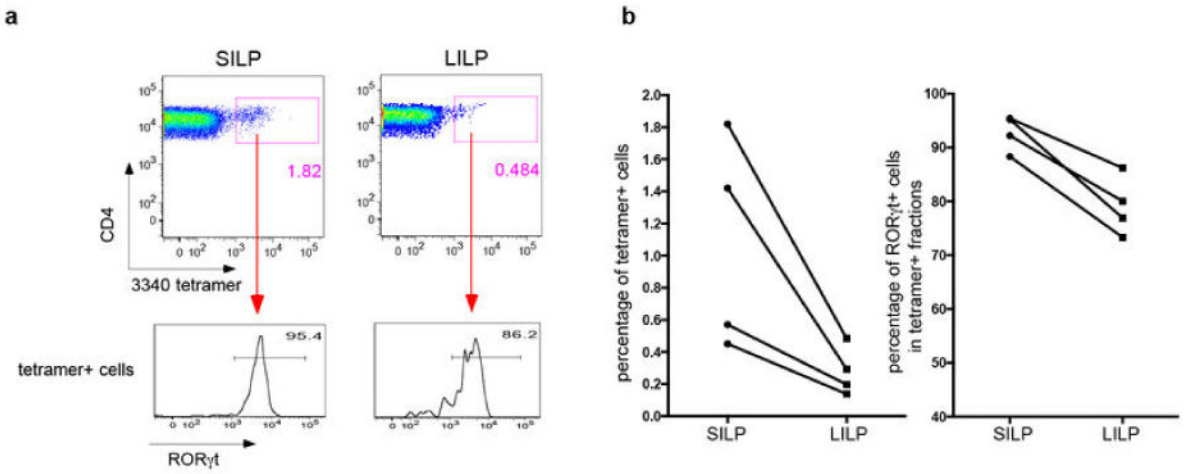

Extended Data Fig. 2. Microbiota-dependent TCR usage bias among SILP Th17 cells

(a) SILP CD4$^+$ T cells from *Il-23r*$^{GFP/+}$ mice were analyzed for utilization of Vβ's in Th17 cells versus non-Th17 cells. Ratios of the percentage of each TCR Vβ in GFP$^+$ vs. GFP$^-$ cells are shown. Each symbol represents one mouse. **(b)** Relative expression of Vβ14 and Vβ6 TCRs by SILP Th17 versus non-Th17 CD4$^+$ T cells from *Il-23r*$^{GFP/+}$ mice. Left: Representative FACS plots; Right: Analysis of multiple animals. **(c)** Specific enrichment of Vβ14 TCRs in CD4$^+$ T cells expressing RORγt and IL-17A, but not FOXP3 or IFNγ. Left: Representative FACS plots. Right: Analysis of multiple animals. Each symbol represents one mouse. **(d)** Correlation of Vβ14 enrichment in Th17 cells with the presence of specific commensal microbiota. B6 Jax mice were housed alone or cohoused with B6 Tac mice for two weeks. Left: Representative FACS analyses. Right: Analysis of multiple animals.

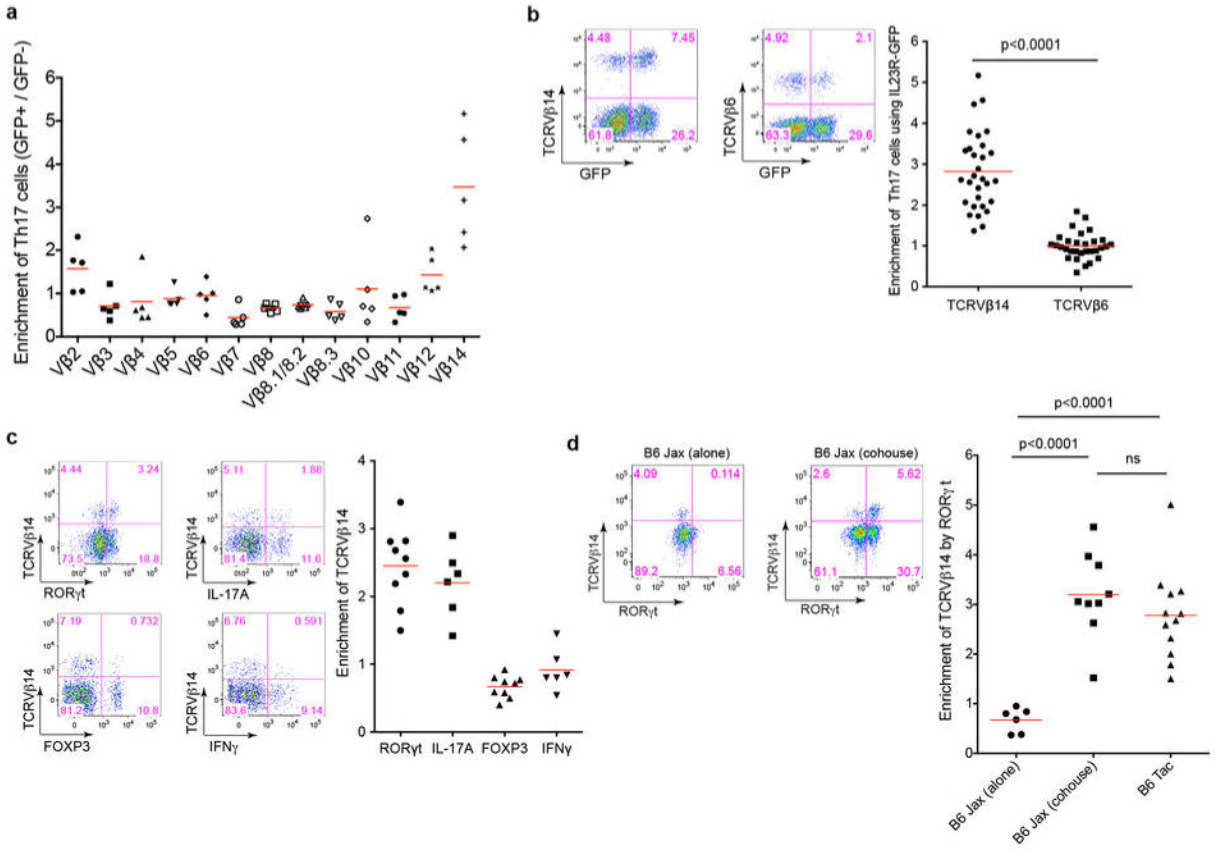

Extended Data Fig. 3. Th17 TCR repertoire analysis by pyrosequencing

(a) Numbers of unique Vβ14 CDR3 sequences of individual SILP Th17 and non-Th17 samples. The sequences were normalized for numbers of cells and total reads. **(b)** Preferential expansion of $V\beta14^{+}$ clones in the Th17 compartment in the SILP. The proportions of the 10 most abundant Vβ14 CDR3 sequences from Th17 and non-Th17 cells from 8 mice are shown. **(c)** Th17-non Th17 bias of unique Vβ14 CDR3 sequences in the SILP of multiple mice.

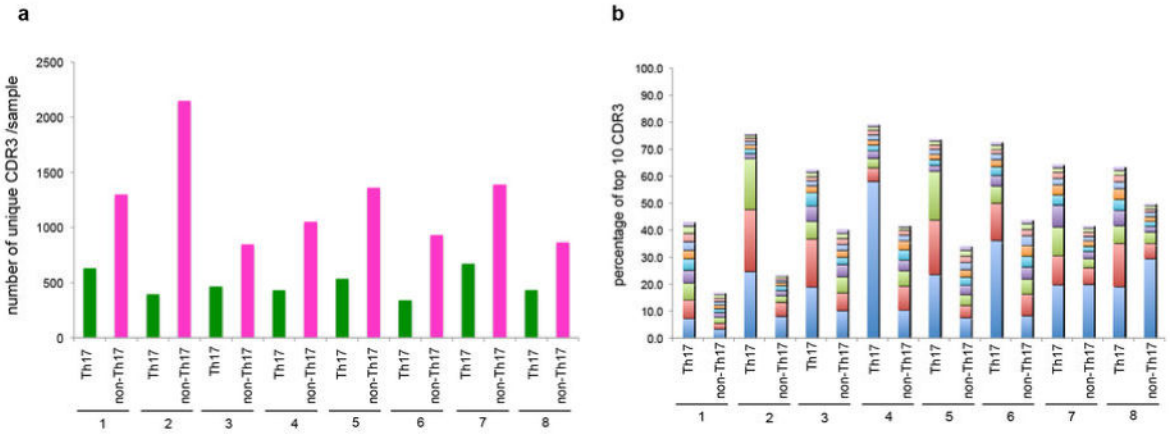

c

	CDR3 (Vβ14)	1		2		3		4		5		6		7		8	
		Th17	non-Th17	Th17	non-Th17	Th17	non-Th17	Th17	non-Th17	Th17	non-Th17	Th17	non-Th17	Th17	non-Th17	Th17	non-Th17
Th17	AWSRGQDTQY	11	0	0	4	319	8	18	2	18	3	0	0	0	0	32	0
	AWSPGLGGYAEQF	49	1	18	0	994	10	0	0	0	0	0	0	0	0	0	0
	AWSLGTGNTEVF	5	0	0	0	5	0	58	1	72	14	169	9	1	0	0	0
	AWSRGTGNTEVF	1	0	77	23	0	0	336	15	163	12	0	0	0	0	0	0
	AWSRGTGDTEVF	0	0	0	0	0	0	140	4	0	0	0	0	805	45	0	0
	AWSLTQPSAETLY	0	0	0	0	0	0	0	0	1307	88	881	89	0	0	0	0
	AWSLQISNERLF	0	0	0	0	0	0	355	14	0	0	0	0	0	1	324	14
	AWSPSASQNTLY	396	13	0	0	363	1	0	0	0	0	0	0	0	0	0	0
	AWSRGTGGNTEVF	265	24	0	0	3	0	0	0	1459	38	0	0	0	0	0	0
	AWSLRVQDTQY	0	0	0	1	99	1	0	0	14	0	0	0	19	2	0	0
	AWSPGTINERLF	361	5	0	0	13	0	0	0	0	0	0	0	0	0	0	0
	AWSPGLGGVCAV	6	0	0	0	85	2	0	0	0	0	0	0	0	0	0	0
	AWSLGVNQDTQY	0	0	0	0	14	0	0	2	0	0	94	11	0	0	0	0
	AWSPGTGGTGQLY	0	0	55	6	0	0	0	0	0	0	0	0	42	0	0	0
	AWSLAISNERLF	0	0	95	41	0	0	0	7	0	2	0	0	0	0	0	0
	AWSLSAETLY	0	1	0	3	0	0	0	0	2	10	0	0	273	120	0	0
	AWSLGTDGNTLY	0	1	0	0	0	0	0	0	0	0	10	270	41	7	0	1
Non-Th17	AWSTGGGQNTLY	0	0	0	0	0	0	0	0	0	0	1	247	30	67	0	0
	AWSLWGSSYEQY	0	57	0	2	0	0	0	0	0	0	0	0	0	0	0	303
	AWSRDRSNSDYT	0	1	0	0	0	6	0	0	3	122	0	0	0	0	0	0
	AWSLEGGEQY	0	66	0	4	0	0	0	0	0	0	0	0	2	6	0	0
	AWSLGFQDTQY	0	99	0	16	0	9	0	0	0	0	0	0	0	0	0	0
	AWSLGLQDTQY	0	158	0	0	0	13	0	0	0	0	0	0	0	0	0	8
	AWSRDWGSQNTLY	0	0	0	0	0	0	0	0	0	487	0	306	0	0	12	1604
	AWSLHSGNTLY	9	99	0	0	3	205	0	0	0	0	0	0	0	0	0	5
	AWSRQQDTQY	0	22	0	0	0	0	0	0	0	9	1	265	0	0	0	6
	AWSLGRANTEVF	0	6	0	0	0	0	0	49	0	11	0	17	0	0	0	0
	AWSRDSQNTLY	6	0	3	46	0	115	0	3	0	0	0	93	0	14	0	0
	AWSRQNSDYT	0	16	0	14	0	0	0	0	0	4	0	18	0	164	0	62

Extended Data Fig. 4. Single-cell TCR cloning and TCR hybridoma screen

(a) Efficiency of single-cell Vβ14 cloning from SILP Th17 and non-Th17 cells of multiple mice. **(b)** Distributions of unique Vβ14 sequences in Th17 and non-Th17 cells within the SILP. Each plot represents one mouse shown in (a). y and x axes represent numbers of Th17 cells and non-Th17 cells for each unique Vβ14 sequence. Numbers of unique sequences are shown in colored circles. **(c)** Responses of Th17 and non-Th17 TCR hybridomas to small intestinal luminal contents from B6 Tac and B6 Jax mice. **(d)** Stimulation of Th17 TCR hybridomas by *SFB*-monoassociated antigens in the presence of APCs sufficient (WT) or deficient (KO) for MHC class II.

a

Mouse	Vβ14+ Th17 cells			Vβ14+ non-Th17 cells			# of cloned CDR3	# of unique CDR3
	# of wells	# of cloned CDR3	Cloning efficiency (%)	# of wells	# of cloned CDR3	Cloning efficiency (%)		
1	84	78	92.8	84	61	72.6	139	57
2	88	80	90.9	88	73	82.9	153	85
3	112	107	95.5	112	91	81.2	198	77
4	112	91	81.2	112	89	79.5	180	85

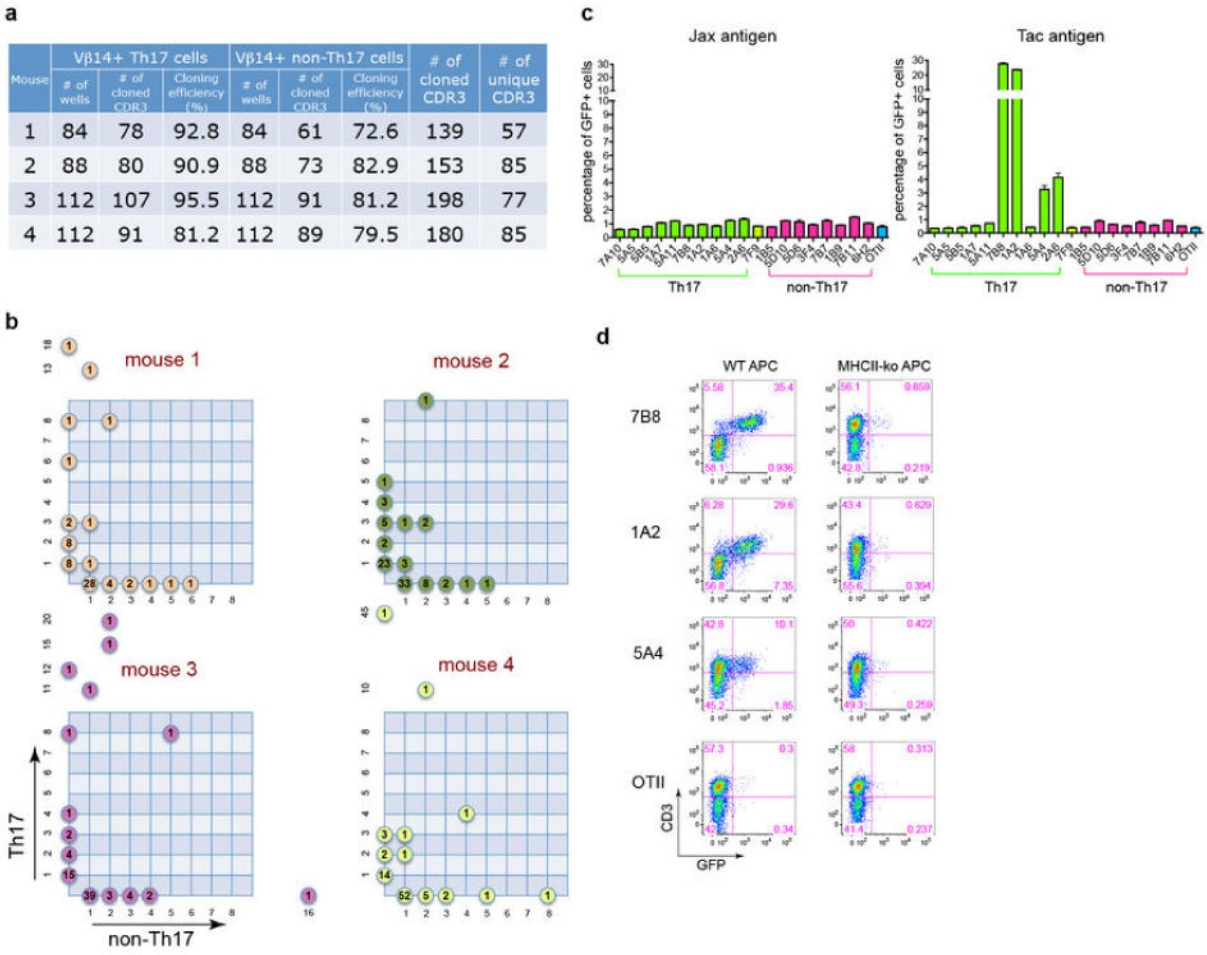

Extended Data Fig. 5. Identification of *SFBNYU_003340* epitopes recognized by a subset of the Th17 TCR hybridomas

(a) Schematic representation of the antigen screen using a whole-genome shotgun *SFB* library. **(b)** Stimulation of the 7B8 hybridoma by bacterial pool 3F12. **(c)** Reactivity of 7B8 and four other TCR hybridomas with bacterial clone *3F12-E8*. **(d)** Diversity of the CDR3 sequences of TCRs specific for *3F12-E8*. Note that they belong to different Vα subsets and have distinct Vβ14 CDR3 sequences. **(e)** Responses of the *3F12-E8*-specific TCR hybridomas to core epitopes encoded by minigenes expressed in *E.coli*.

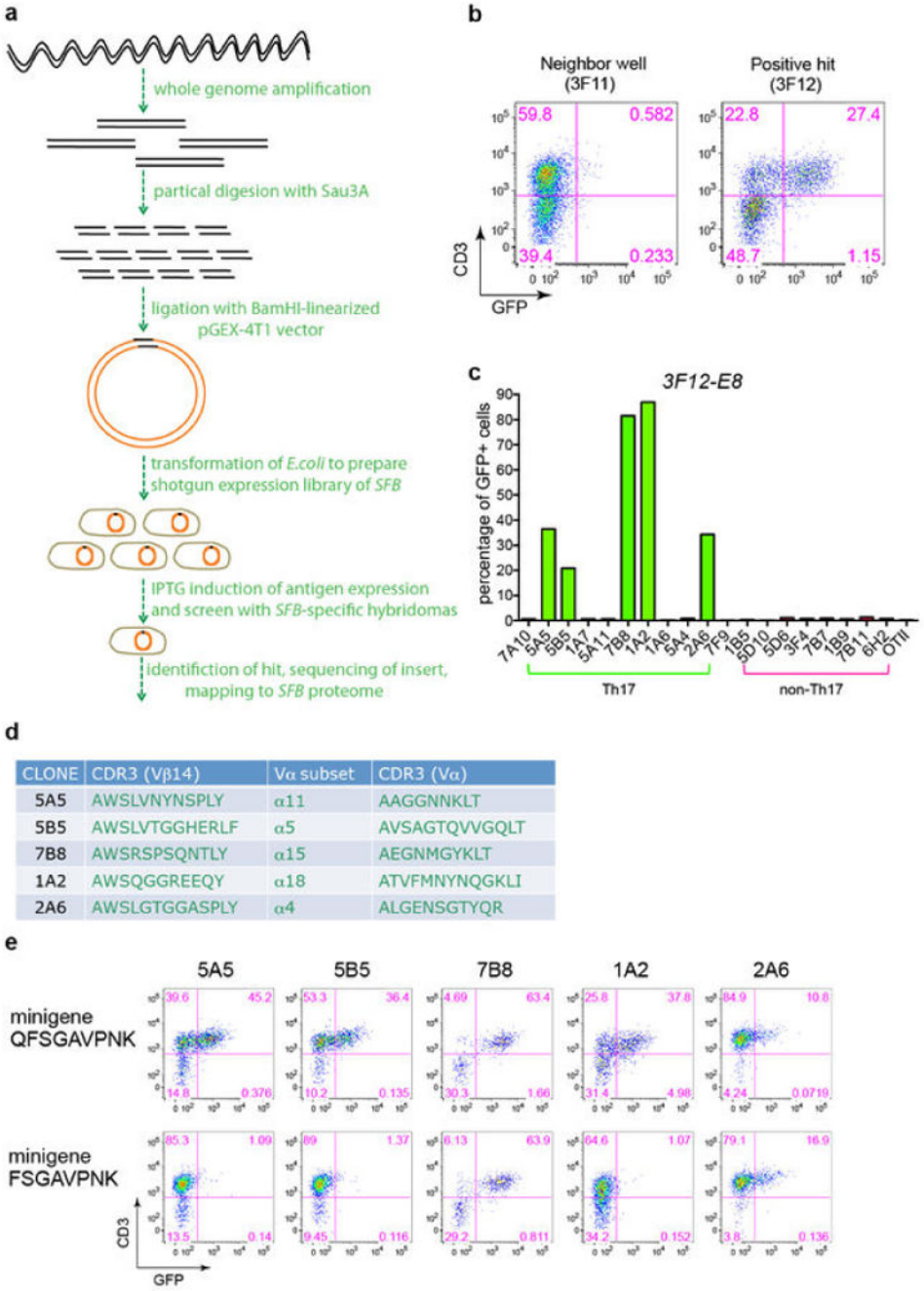

Extended Data Fig. 6. Identification of *SFBNYU_004990* epitopes recognized by related TCRs

(a) Top: The distribution in Th17 and non-Th17 cells of four TCRs that share an identical TCRα chain. Bottom: Amino acid alignment of the Vβ14 CDR3 sequences. The green box highlights the sequence differences. **(b)** Stimulation of the 5A11 hybridoma by bacterial pool 2D10 in the *SFB* antigen screen. **(c)** Responses of 4 TCR hybridomas, including a non-Th17 hybridoma, to bacterial clone *2D10-A10*. **(d)** Responses of the *2D10-A10*-specific TCR hybridomas to core epitopes encoded by minigenes expressed in *E.coli*. **(e)** TCR

hybridoma responses to titrated synthetic peptide (IRWFGSSVQKV) in the presence of APCs.

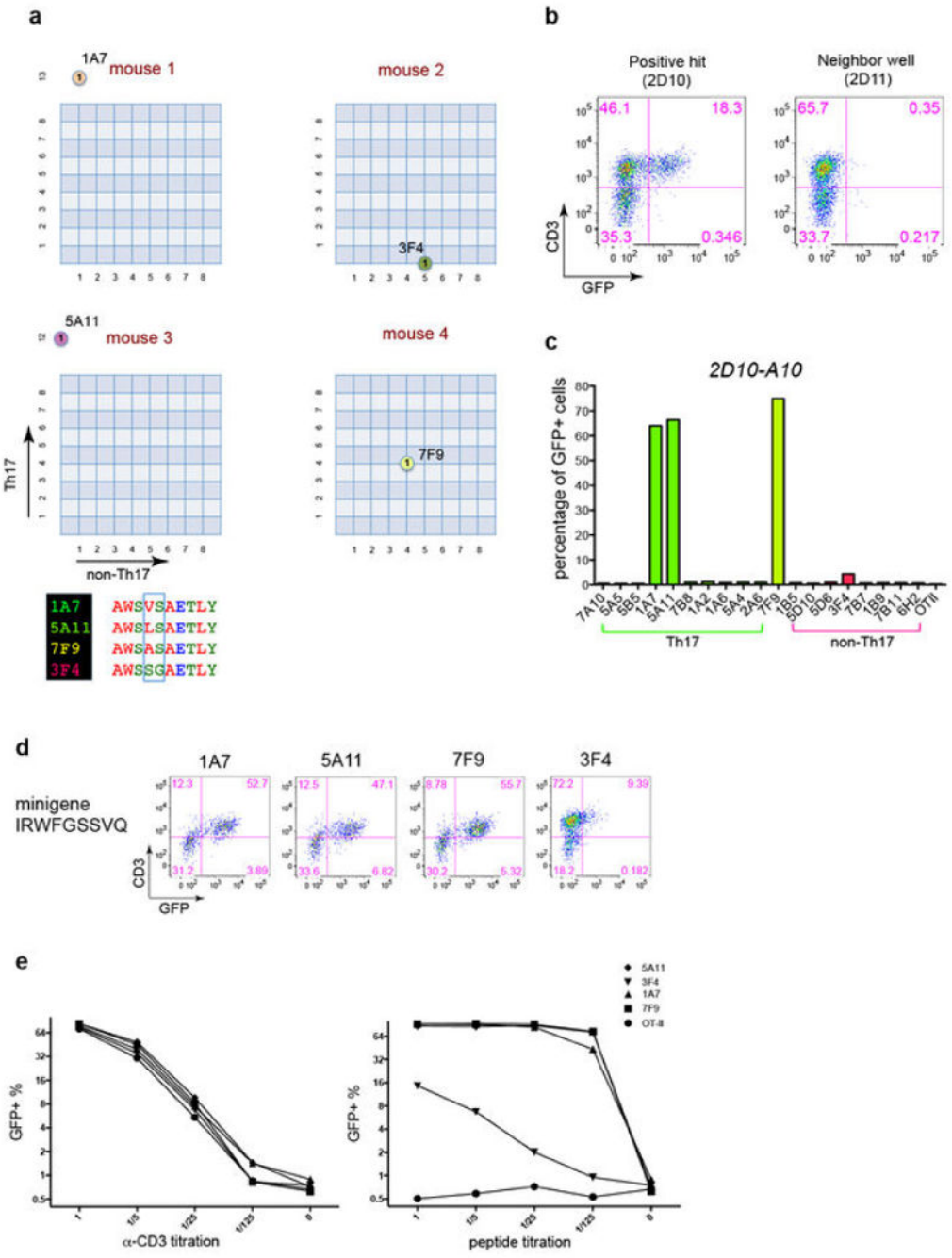

Extended Data Fig. 7. *SFB* epitopes recognized by diverse Th17 cell TCRs

(a) The epitopes recognized by the Vβ14^{+} TCR hybridomas stimulate only Vβ14^{+} Th17 cells from the SILP. Th17 cells sorted from *Il-23r*$^{GFP/+}$ mice were stimulated with indicated peptides (listed in (d)) in the presence of APCs. Left: Representative IL-17A ELISPOT assay with triplicates. Right: Normalized peptide-specific Th17 responses. Each dot

represents one mouse. **(b)** Polyclonal responses of Vβ14^{+} and Vβ14^{-} SILP Th17 cells to *SFB* antigens. Representative FACS plots from five experiments are shown. **(c)** Bioinformatics filtering approach to select candidate *SFB* epitopes. **(d)** Summary of newly-selected and the known A6 and A15 *SFB* peptides. **(e)** IL-17A ELISPOT screen for indicated peptides using SILP Th17 cells sorted from *SFB*-colonized *Il-23r*$^{GFP/+}$ mice. The A6 peptide from *SFBNYU_003340* and anti-CD3 served as positive controls. **(f)** Vβ14 usage in Th17 cells specific for peptide N5. Left: Representative IL-17A ELISPOT assay with triplicates for peptide N5, using Vβ14^{+} and Vβ14^{-} SILP Th17 cells sorted from *Il-23r*$^{GFP/+}$ mice. Right: Normalized N5-specific Th17 responses. Each dot represents one mouse.

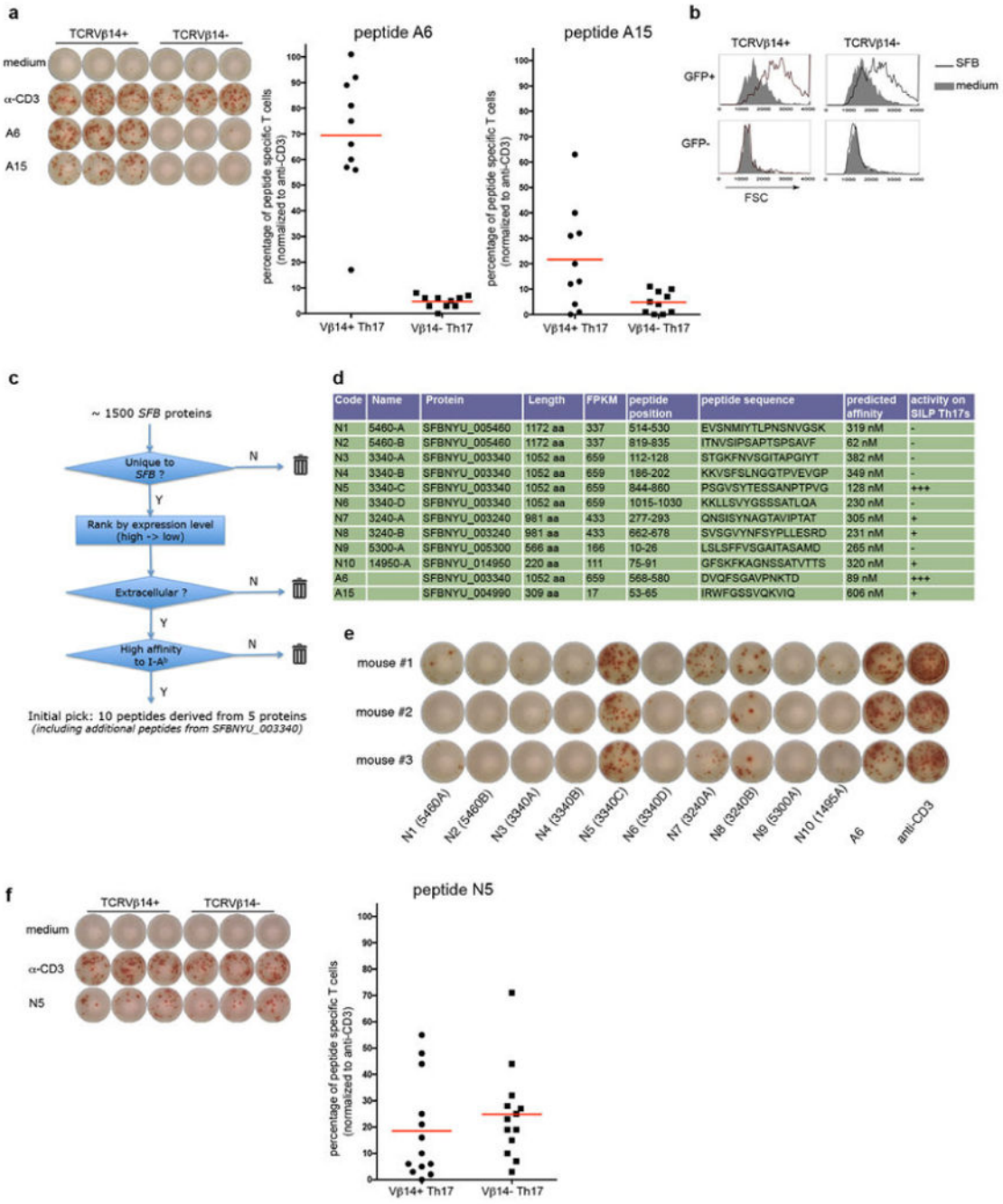

Code	Name	Protein	Length	FPKM	peptide position	peptide sequence	predicted affinity	activity on SILP Th17s
N1	5460-A	SFBNYU_005460	1172 aa	337	514-530	EVSNMIYTLPNSNVGSK	319 nM	-
N2	5460-B	SFBNYU_005460	1172 aa	337	819-835	ITNVSIPSAPTSPSAVF	62 nM	-
N3	3340-A	SFBNYU_003340	1052 aa	659	112-128	STGKFNVSGITAPGIYT	382 nM	-
N4	3340-B	SFBNYU_003340	1052 aa	659	186-202	KKVSFSLNGGTPVEVGP	349 nM	-
N5	3340-C	SFBNYU_003340	1052 aa	659	844-860	PSGVSYTESSANPTPVG	128 nM	+++
N6	3340-D	SFBNYU_003340	1052 aa	659	1015-1030	KKLLSVYGSSSATLQA	230 nM	-
N7	3240-A	SFBNYU_003240	981 aa	433	277-293	QNSISYNAGTAVIPTAT	305 nM	+
N8	3240-B	SFBNYU_003240	981 aa	433	662-678	SVSGVYNFSYPLLESRD	231 nM	+
N9	5300-A	SFBNYU_005300	566 aa	166	10-26	LSLSFFVSGAITASAMD	265 nM	-
N10	14950-A	SFBNYU_014950	220 aa	111	75-91	GFSKFKAGNSSATVTTS	320 nM	+
A6		SFBNYU_003340	1052 aa	659	568-580	DVQFSGAVPNKTD	89 nM	+++
A15		SFBNYU_004990	309 aa	17	53-65	IRWFGSSVQKVIQ	606 nM	+

Extended Data Fig. 8. *SFB*-specific T cells become Th17 cells in *SFB*-colonized mice

(a) *SFB*-dependent *7B8Tg* T cell accumulation in the SILP. 2×10^4 naive *7B8Tg* T cells were transferred into congenic Ly5.1 recipient mice that were *SFB*-colonized or *SFB*-free. $CD4^+$ T cells in the SILP were examined for donor and recipient isotype markers after 13 days. **(b)** Top: Strategy for co-transfer of congenic *1A2Tg* and *5A11Tg* T cells into *SFB*-colonized recipient mice. Bottom: FACS analysis of RORγt expression in host- and donor-derived $CD4^+$ T cells in the SILP at 7 days after transfer. **(c)** FACS analysis of transcription factors in host- and donor- derived SILP $CD4^+$ T cells after transfer of naïve *7B8Tg* T cells as in (a).

(d) FACS analysis of SILP T cells from *Il-23r*$^{GFP/+}$ mice, stained with I-A^{b}/3340-A6 tetramer and control tetramer (2W). **(e)** FACS analysis of SILP T cells of B6 mice from colonies with different microbiota, stained with I-A^{b}/3340-A6 tetramer and intracellular RORγt antibody. **(f)** Expansion of *7B8Tg* T cells in mice colonized with *Listeria monocytogenes* expressing *SFBNYU_003340*. Top: Immunofluorescence microscopic visualization of the expression of *SFB* protein by *L. monocytogenes*. *Listeria-3340* and *Listeria-empty* were stained with anti-3340 rabbit polyclonal antibody. Red: anti-3340 antibody staining. Blue: DAPI staining. Bottom: Naive Ly5.1^{+} *7B8Tg* cells were transferred into congenic mice infected with *Listeria-3340* or *Listeria-empty*. Seven days after transfer, donor derived CD4^{+} T cells in the SILP were analyzed by FACS.

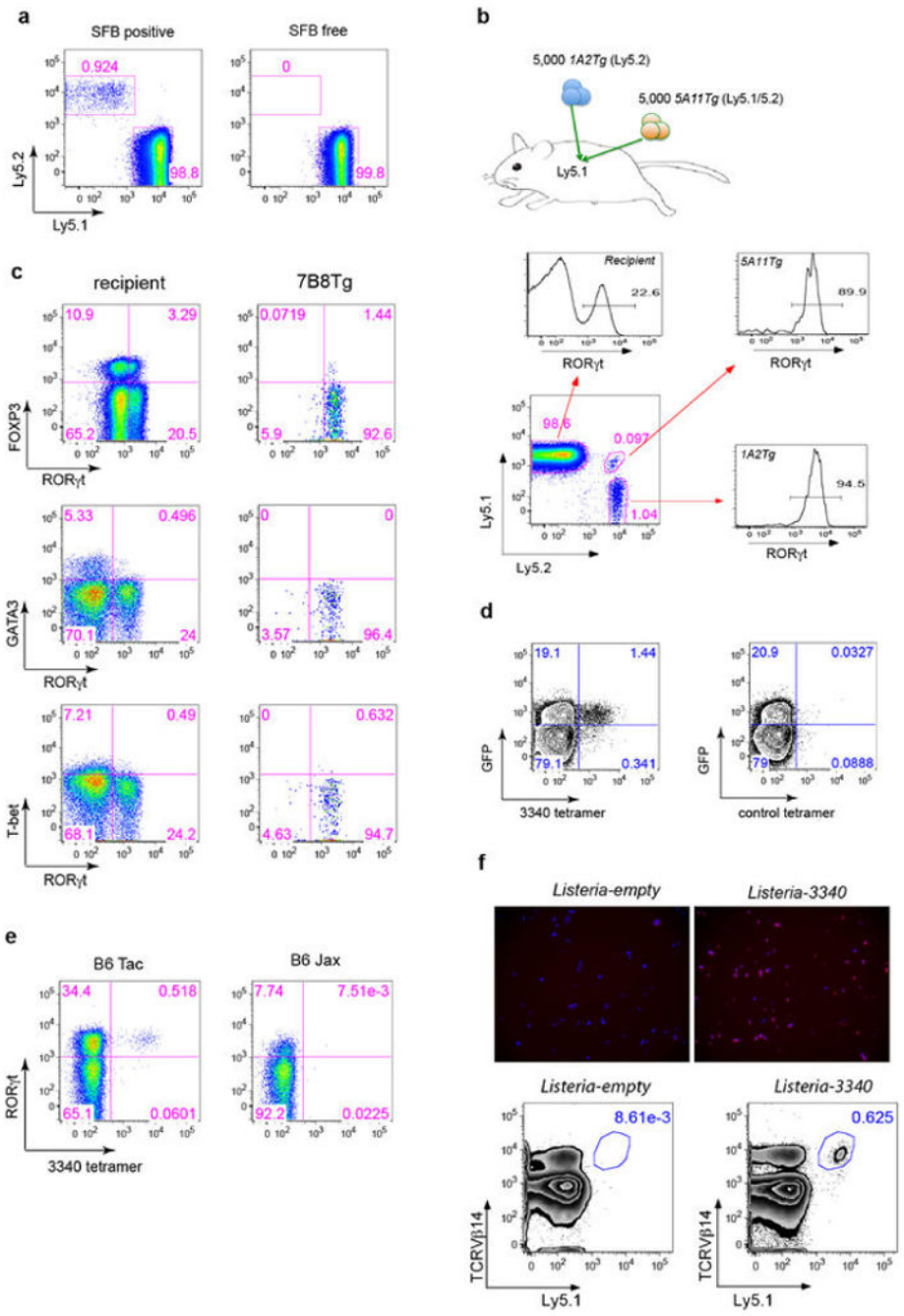

Extended Data Fig. 9. Transcription factor expression in *SFB*-specific and *Listeria*-specific T cells in co-infected mice (representative of data plotted in Fig. 4b)

(a) Experimental design for tracking both *SFB*- and *Listeria*- specific CD4$^+$ T cells following intestinal colonization with both bacteria. Ly5.2 B6 mice were colonized with *Listeria monocytogenes*, *SFB*, or both bacteria, and *7B8Tg* T cells from Ly5.1 mice were injected IV. Expression of Th1 and Th17 transcription factors in the *SFB*-specific *7B8Tg* cells and LLO tetramer-specific recipient T cells was evaluated. **(b)** Intracellular stain for RORγt. **(c)** Intracellular stain for T-bet.

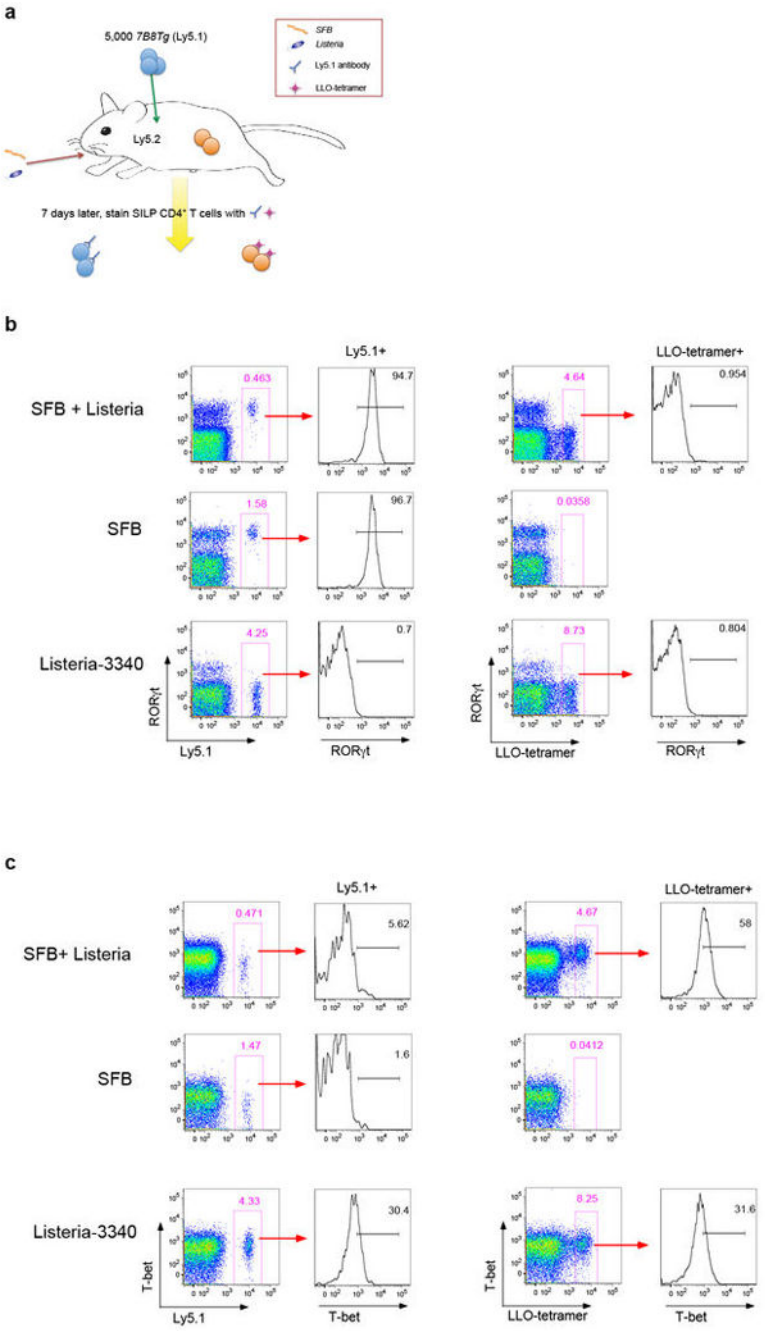

Extended Data Fig. 10. *SFB*-specific Th17 cells are present in both SILP and LILP of *SFB*-colonized mice

T cells were stained with I-A^b/3340-A6 tetramer and antibody to intracellular RORγt. **(a)** Representative FACS plots (gated on $CD4^+$ T cells). **(b)** Analysis of multiple animals. Left: percent of tetramer-positive cells among total $CD4^+$ T cells in each region of the intestine. Right: percent of RORγt$^+$ cells among the tetramer-positive cells. Each symbol represents cells from a separate animal.

Supplementary Material

Refer to Web version on PubMed Central for supplementary material.

Acknowledgments

We thank Dr. Sang Yong Kim in the Rodent Genetic Engineering Core (NYU) for generating TCR transgenic mice; Dr. Debra Morrison in the Immune Monitoring Core (NYU), which is supported in part by grant UL1 TR00038 from the National Center for Advancing Translational Sciences and grant 5P30CA016087-32 from the National Cancer Institute; the NYU Histology Core which is supported in part by grant 5P30CA016087-32 from the National Cancer Institute; Dr. Agnes Viale in the Genomics Core Laboratory (MSKCC) for 454 pyrosequencing; Dr. Richard Myers at the HudsonAlpha Institute of Biotechnology for RNA-seq; Dr. Nancy Freitag (University of Illinois at Chicago) for providing the Listeria strain and expression vector; Dr. Yoshinori Umesaki (Yakult) for SFB samples; and Dr. Kenneth Murphy (Washington University, St. Louis) for providing the 58$\alpha^{-}\beta^{-}$ hybridoma line. Y.Y. was supported by the Arthritis National Research Foundation. M.X. is supported by the Irvington Institute fellowship program of the Cancer Research Institute. D.R.L. is a Howard Hughes Medical Institute Investigator.

References

1. Bettelli E, Korn T, Oukka M, Kuchroo VK. Induction and effector functions of T(H)17 cells. Nature. 2008; 453:1051–1057.10.1038/nature07036 [PubMed: 18563156]
2. McGeachy MJ, Cua DJ. The link between IL-23 and Th17 cell-mediated immune pathologies. Seminars in immunology. 2007; 19:372–376.10.1016/j.smim.2007.10.012 [PubMed: 18319054]
3. Littman DR, Rudensky AY. Th17 and regulatory T cells in mediating and restraining inflammation. Cell. 2010; 140:845–858.10.1016/j.cell.2010.02.021 [PubMed: 20303875]
4. Ivanov II, et al. The orphan nuclear receptor RORgammat directs the differentiation program of proinflammatory IL-17+ T helper cells. Cell. 2006; 126:1121–1133.10.1016/j.cell.2006.07.035 [PubMed: 16990136]
5. Ivanov II, et al. Specific microbiota direct the differentiation of IL-17-producing T-helper cells in the mucosa of the small intestine. Cell host & microbe. 2008; 4:337–349.10.1016/j.chom.2008.09.009 [PubMed: 18854238]
6. Atarashi K, et al. ATP drives lamina propria T(H)17 cell differentiation. Nature. 2008; 455:808–812.10.1038/nature07240 [PubMed: 18716618]
7. Atarashi K, et al. Treg induction by a rationally selected mixture of Clostridia strains from the human microbiota. Nature. 201310.1038/nature12331
8. Ivanov II, et al. Induction of intestinal Th17 cells by segmented filamentous bacteria. Cell. 2009; 139:485–498.10.1016/j.cell.2009.09.033 [PubMed: 19836068]
9. Gaboriau-Routhiau V, et al. The key role of segmented filamentous bacteria in the coordinated maturation of gut helper T cell responses. Immunity. 2009; 31:677–689.10.1016/j.immuni.2009.08.020 [PubMed: 19833089]
10. Wu HJ, et al. Gut-residing segmented filamentous bacteria drive autoimmune arthritis via T helper 17 cells. Immunity. 2010; 32:815–827.10.1016/j.immuni.2010.06.001 [PubMed: 20620945]
11. Lee YK, Menezes JS, Umesaki Y, Mazmanian SK. Proinflammatory T-cell responses to gut microbiota promote experimental autoimmune encephalomyelitis. Proceedings of the National Academy of Sciences of the United States of America. 2011; 108(Suppl 1):4615–4622.10.1073/pnas.1000082107 [PubMed: 20660719]
12. Ivanov II, Honda K. Intestinal commensal microbes as immune modulators. Cell host & microbe. 2012; 12:496–508.10.1016/j.chom.2012.09.009 [PubMed: 23084918]
13. Hooper LV, Littman DR, Macpherson AJ. Interactions between the microbiota and the immune system. Science. 2012; 336:1268–1273.10.1126/science.1223490 [PubMed: 22674334]
14. Schnupf P, Gaboriau-Routhiau V, Cerf-Bensussan N. Host interactions with Segmented Filamentous Bacteria: An unusual trade-off that drives the post-natal maturation of the gut immune system. Seminars in immunology. 2013; 25:342–351.10.1016/j.smim.2013.09.001 [PubMed: 24184014]

15. Lochner M, et al. Restricted microbiota and absence of cognate TCR antigen leads to an unbalanced generation of Th17 cells. J Immunol. 2011; 186:1531–1537.10.4049/jimmunol.1001723 [PubMed: 21178008]
16. Awasthi A, et al. Cutting edge: IL-23 receptor gfp reporter mice reveal distinct populations of IL-17-producing cells. J Immunol. 2009; 182:5904–5908.10.4049/jimmunol.0900732 [PubMed: 19414740]
17. Ise W, et al. CTLA-4 suppresses the pathogenicity of self antigen-specific T cells by cell-intrinsic and cell-extrinsic mechanisms. Nature immunology. 2010; 11:129–135.10.1038/ni.1835 [PubMed: 20037585]
18. Sanderson S, Campbell DJ, Shastri N. Identification of a CD4+ T cell-stimulating antigen of pathogenic bacteria by expression cloning. The Journal of experimental medicine. 1995; 182:1751–1757. [PubMed: 7500019]
19. Sczesnak A, et al. The genome of th17 cell-inducing segmented filamentous bacteria reveals extensive auxotrophy and adaptations to the intestinal environment. Cell host & microbe. 2011; 10:260–272.10.1016/j.chom.2011.08.005 [PubMed: 21925113]
20. Prakash T, et al. Complete genome sequences of rat and mouse segmented filamentous bacteria, a potent inducer of th17 cell differentiation. Cell host & microbe. 2011; 10:273–284.10.1016/j.chom.2011.08.007 [PubMed: 21925114]
21. Kouskoff V, Signorelli K, Benoist C, Mathis D. Cassette vectors directing expression of T cell receptor genes in transgenic mice. Journal of immunological methods. 1995; 180:273–280. [PubMed: 7714342]
22. Kearney ER, Pape KA, Loh DY, Jenkins MK. Visualization of peptide-specific T cell immunity and peripheral tolerance induction in vivo. Immunity. 1994; 1:327–339. [PubMed: 7889419]
23. Moon JJ, et al. Naive CD4(+) T cell frequency varies for different epitopes and predicts repertoire diversity and response magnitude. Immunity. 2007; 27:203–213.10.1016/j.immuni.2007.07.007 [PubMed: 17707129]
24. Hsieh CS, et al. Development of TH1 CD4+ T cells through IL-12 produced by Listeria-induced macrophages. Science. 1993; 260:547–549. [PubMed: 8097338]
25. Hand TW, et al. Acute gastrointestinal infection induces long-lived microbiota-specific T cell responses. Science. 2012; 337:1553–1556.10.1126/science.1220961 [PubMed: 22923434]
26. Scher JU, et al. Expansion of intestinal Prevotella copri correlates with enhanced susceptibility to arthritis. eLife. 2013; 2:e01202.10.7554/eLife.01202 [PubMed: 24192039]
27. Monk IR, Gahan CG, Hill C. Tools for functional postgenomic analysis of listeria monocytogenes. Applied and environmental microbiology. 2008; 74:3921–3934.10.1128/AEM.00314-08 [PubMed: 18441118]
28. Xayarath B, Marquis H, Port GC, Freitag NE. Listeria monocytogenes CtaP is a multifunctional cysteine transport-associated protein required for bacterial pathogenesis. Molecular microbiology. 2009; 74:956–973.10.1111/j.1365-2958.2009.06910.x [PubMed: 19818015]
29. Alamyar E, Giudicelli V, Li S, Duroux P, Lefranc MP. IMGT/HighV-QUEST: the IMGT(R) web portal for immunoglobulin (IG) or antibody and T cell receptor (TR) analysis from NGS high throughput and deep sequencing. Immunome research. 2012; 8:26.
30. Currier, JR.; Robinson, MA. Spectratype/immunoscope analysis of the expressed TCR repertoire. In: Coligan, John E., et al., editors. Current protocols in immunology. Vol. Chapter 10. 2001. p. 28
31. Langmead B, Trapnell C, Pop M, Salzberg SL. Ultrafast and memory-efficient alignment of short DNA sequences to the human genome. Genome biology. 2009; 10:R25.10.1186/gb-2009-10-3-r25 [PubMed: 19261174]
32. Roberts A, Pimentel H, Trapnell C, Pachter L. Identification of novel transcripts in annotated genomes using RNA-Seq. Bioinformatics. 2011; 27:2325–2329.10.1093/bioinformatics/btr355 [PubMed: 21697122]
33. Tubo NJ, et al. Single naive CD4+ T cells from a diverse repertoire produce different effector cell types during infection. Cell. 2013; 153:785–796.10.1016/j.cell.2013.04.007 [PubMed: 23663778]
34. Lauer P, Chow MY, Loessner MJ, Portnoy DA, Calendar R. Construction, characterization, and use of two Listeria monocytogenes site-specific phage integration vectors. Journal of bacteriology. 2002; 184:4177–4186. [PubMed: 12107135]

35. Yu NY, et al. PSORTb 3.0: improved protein subcellular localization prediction with refined localization subcategories and predictive capabilities for all prokaryotes. Bioinformatics. 2010; 26:1608–1615.10.1093/bioinformatics/btq249 [PubMed: 20472543]

36. Yu CS, Chen YC, Lu CH, Hwang JK. Prediction of protein subcellular localization. Proteins. 2006; 64:643–651.10.1002/prot.21018 [PubMed: 16752418]

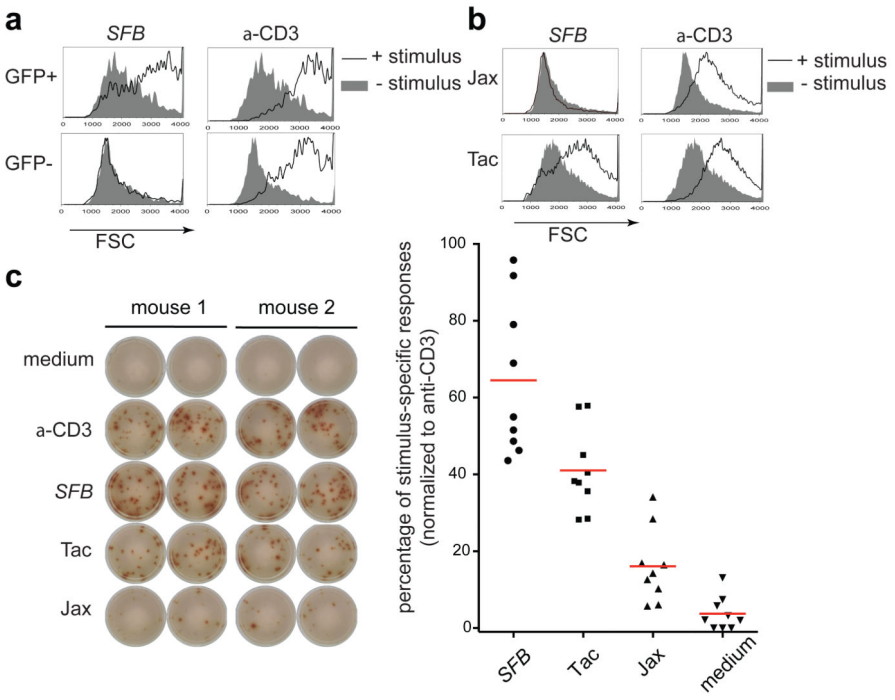

Fig. 1. Intestinal Th17 cells are specific for *SFB*- and other microbiota-derived antigens

(a) Selective activation of intestinal GFP$^+$ CD4$^+$ T cells from *Il-23r*$^{GFP/+}$ mice by fecal extract from *SFB*-monoassociated mice. Forward scatter (FSC) was evaluated after 2 days. **(b)** Activation of SILP CD4$^+$ T cells from B6 Tac mice and B6 Jax mice with fecal extract from *SFB*-monoassociated mice. **(c)** IL17A ELISPOT assay of intestinal GFP$^+$ CD4$^+$ T cells from *SFB*-colonized *Il-23r*$^{GFP/+}$ mice treated with indicated stimuli. Left: Representative ELISPOT images. Right: Compilation of results from multiple animals. Each symbol represents cells from a separate animal.

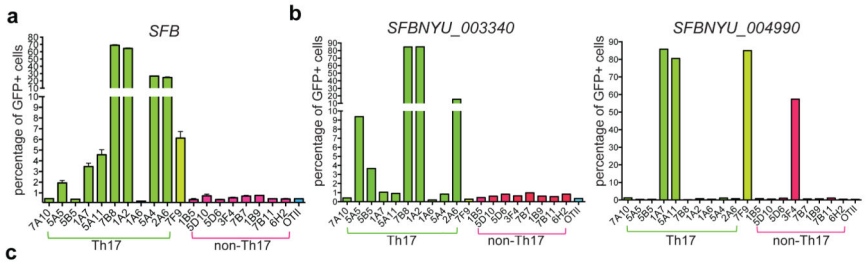

Clone	Mouse	CDR3 (Vβ14)	# of Th17	# of non -Th17	# of TCRα	Vα subset	CDR3 (Vα)	TCR epitope mapped
7A10	4	AWSRDRGQNTLY	45		38	α2	AASGRNNNAPR	
5A5	3	AWSLVNYNSPLY	20	2	10	α11	AAGGNNKLT	QFSGAVPNK
5B5	3	AWSLVTGGHERLF	15	2	7	α5	AVSAGTQVVGQLT	QFSGAVPNK
1A7	1	AWSVSAETLY	13	1	12	α18	ATGGTGYQNFY	IRWFGSSVQ
5A11	3	AWSLSAETLY	12		10	α18	ATGGTGYQNFY	IRWFGSSVQ
7B8	4	AWSRSPSQNTLY	10	2	4	α15	AEGNMGYKLT	FSGAVPNK
1A2	1	AWSQGGREEQY	8	2	9	α18	ATVFMNYNQGKLI	QFSGAVPNK
1A6	1	AWNGAYAEQF	8		6	α5	AVTLNNAGAKLT	
5A4	3	AWSQKGVGANSDYT	8		8	α18	ATTLGQGKLI	(unknown in *SFB*)
2A6	1	AWSLGTGGASPLY	6		6	α4	ALGENSGTYQR	FSGAVPNK
7F9	4	AWSASAETLY	4	4	8	α18	ATGGTGYQNFY	IRWFGSSVQ
1B5	1	AWSLGWGYTGQLY		4	4	α8	ALRGTEGADRLT	
5D10	3	AWSQGTINTEVF		4	3	α18	ATDANSGTYQR	
5D6	3	AWSLTGLNYAEQF		4	3	α18	ATGGANTGKLT	
3F4	2	AWSSGAETLY		5	5	α18	ATGGTGYQNFY	IRWFGSSVQ
7B7	4	AWSLGLQDTQY		5	4	α20	AAGTNYGNEKIT	
1B9	1	AWSPSGGPQDTQY		6	6	α18	APMSNYNVLY	
7B11	4	AWSLQNTGQLY		8	3	α2	AAIGGGGSAKLI	
6H2	3	AWSRDIQDTQY		16	7	α4	ALVDEGTGGYKVV	

Antigen	*SFBNYU_003340*	*SFBNYU_004990*
Size	1050 aa	309 aa
Annotation	hypothetical protein	hypothetical protein
Function	unknown	unknown
Unique to *SFB*	yes	yes
Expression (*RNAseq*)	659 fpkm	17 fpkm
Epitope affinity to I-A^b *(predicted)*	89 nM	606 nM
Localization *(predicted)*	extracellular	extracellular

Fig. 2. Most Th17 TCR hybridomas recognize *SFB*-unique proteins

(a) Responses of the TCR hybridomas, prepared from Th17 and non-Th17 intestinal CD4$^+$ T cells, to fecal material from *SFB*-monoassociated mice. **(b)** Responses of the TCR hybridomas to *E.coli* clones expressing full-length *SFBNYU_003340* and *SFBNYU_004990*. Note that a non-Th17 TCR hybridoma also responded to the clone expressing *SFBNYU_004990*. **(c)** Summary of the nineteen dominant clonotypic TCR clones. Ten Th17-biased clones are highlighted in green, and eight non-Th17-biased clones are highlighted in red. **(d)** Features of the two antigenic proteins of *SFB*.

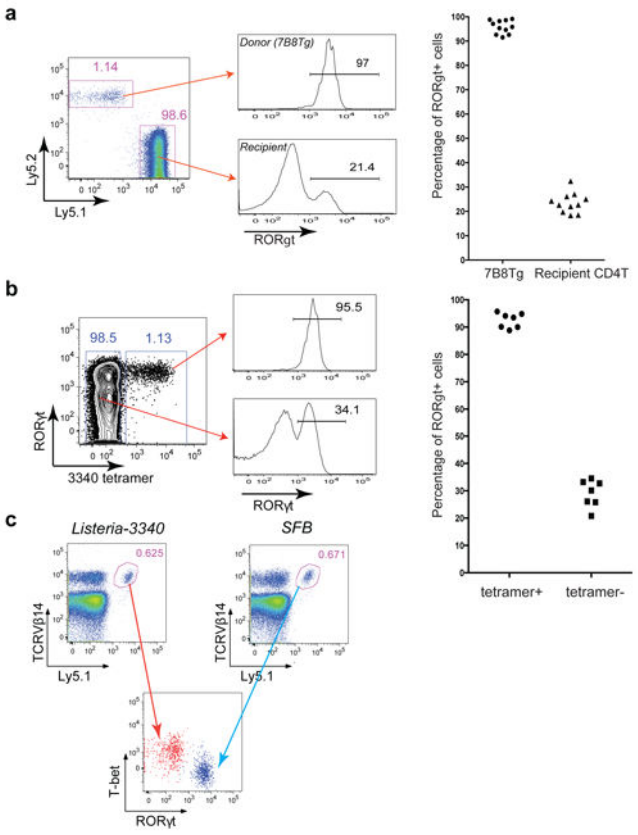

Fig. 3. *SFB*-specific T cells become Th17 cells in the SILP

(a) *7B8Tg* cells (Ly5.2) were transferred into *SFB*-colonized mice (Ly5.1), and SILP T cells were analyzed after 8-15 days. Left: Representative FACS plots. Right: Analysis of multiple animals (one symbol/animal). **(b)** I-A^b/3340-A6 tetramer stain of SILP T cells from *SFB*-colonized B6 mice. Left: Representative FACS plots. Right: Analysis of multiple animals (one symbol/animal). **(c)** *7B8Tg* cells (Ly5.1) were transferred into Ly5.2 congenic hosts orally colonized with *Listeria-3340* or *SFB*. Seven days after transfer, donor-derived cells in the SILP were analyzed. The results are representative of three experiments.

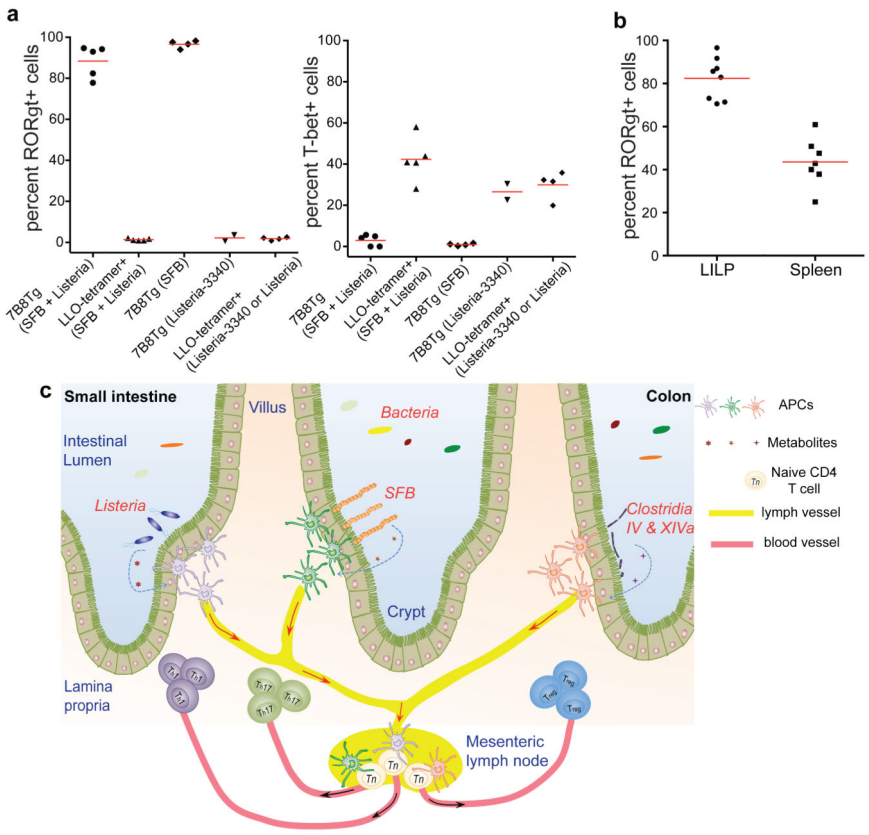

Fig. 4. TCR specificity for distinct luminal bacteria underlies divergent T helper cell differentiation in the SILP

(a) Th17 (RORγt) versus Th1 (T-bet) differentiation of *SFB*- (*7B8Tg*) and *Listeria* (LLO-tetramer)-specific $CD4^+$ T cells in mice colonized with either or both bacteria. Each symbol represents cells from one animal. **(b)** Proportions of donor-derived *7B8Tg* T cells that express RORγt in the colon and spleen of *SFB*-colonized mice. **(c)** Model for intestinal niches that promote diverse microbiota-dependent $CD4^+$ effector T cell programs. Microbial signals, may induce polarizing cytokines or preformed niche-specific antigen presenting cells may interact with different T cell-inducing bacteria.